

1 **Delayed APC/C activation extends the first mitosis of mouse embryos**

2 Anna Ajduk<sup>1,2</sup>, Bernhard Strauss<sup>1</sup>, Jonathon Pines<sup>1,3,\*</sup>, Magdalena Zernicka-Goetz<sup>1,4,\*</sup>

3

4

5 <sup>1</sup>The Wellcome Trust/Cancer Research UK Gurdon Institute, University of Cambridge, Tennis  
6 Court Road, CB2 1QN, UK

7 <sup>2</sup>Department of Embryology, Faculty of Biology, University of Warsaw, Miecznikowa 1, 02-  
8 096 Warsaw, Poland

9 <sup>3</sup>The Institute of Cancer Research, 237 Fulham Road, London SW3 6JB, UK

10 <sup>4</sup>Department of Physiology, Development and Neuroscience, University of Cambridge,  
11 Downing Street, Cambridge CB2 3GE, UK

12 \*Co-corresponding authors:

13 Jonathon Pines,

14 Jon.pines@icr.ac.uk

15 and

16 Magdalena Zernicka-Goetz,

17 mz205@cam.ac.uk

18

19

20

21

22 The correct temporal regulation of mitosis underpins genomic stability because it ensures  
23 the alignment of chromosomes on the mitotic spindle that is required for their proper  
24 segregation to the two daughter cells. Crucially, sister chromatid separation must be  
25 delayed until all the chromosomes have attached to the spindle; this is achieved by the  
26 Spindle Assembly Checkpoint (SAC) that inhibits the Anaphase Promoting  
27 Complex/Cyclosome (APC/C) ubiquitin ligase. In many species the first embryonic M-phase  
28 is significantly prolonged compared to the subsequent divisions, but the reason behind this  
29 has remained unclear. Here, we show that the first M-phase in the mouse embryo is  
30 significantly extended due to a delay in APC/C activation. Unlike in somatic cells, where the  
31 APC/C first targets cyclin A2 for degradation at nuclear envelope breakdown (NEBD), we find  
32 that in zygotes cyclin A2 remains stable for a significant period of time after NEBD. Our  
33 findings that the SAC prevents cyclin A2 degradation, whereas over-expressed Plk1  
34 stimulates it, support our conclusion that the delay in cyclin A2 degradation is caused by low  
35 APC/C activity. As a consequence of delayed APC/C activation cyclin B1 stability in the first  
36 mitosis is also prolonged, leading to the unusual length of the first M-phase.

37

38

39

40

41

42

43

44

## 45 Introduction

46 The time between NEBD and the onset of anaphase is one of the most important periods for  
47 genomic stability as the cell must ensure that all the chromosomes are attached to the  
48 mitotic spindle before sister chromatids separate. This is achieved by regulating the activity  
49 of the key ubiquitin-ligase in mitosis, APC/C. In a typical mitotic division, the APC/C is  
50 activated at NEBD and one of its first substrates is cyclin A2<sup>1,2</sup>. Cyclin A2 is required for cells  
51 to enter M-phase and it is targeted by the APC/C even though the SAC is active, monitoring  
52 unattached chromosomes<sup>3,4</sup>, and generating the Mitotic Checkpoint Complex (MCC) that  
53 inhibits the APC/C. Cyclin A2 can be degraded when the SAC is active because it can  
54 compete with the MCC component, BubR1, to bind Cdc20<sup>5</sup>. The cyclin A2-Cdc20 complex  
55 then binds to the APC/C through a Cks protein<sup>6,7</sup>. This mode of recognition allows cyclin A2  
56 to be preferentially ubiquitylated by the APC/C over securin and cyclin B1, when APC/C  
57 activity is limited<sup>8</sup>.

58 By contrast, the timing of cyclin B1 and securin degradation is controlled by the SAC, which  
59 prevents the APC/C from recognising cyclin B1 and securin by inactivating Cdc20. One  
60 molecule of Cdc20 is incorporated into a complex with the Mad2, BubR1 and Bub3 proteins  
61 to form the MCC that itself can inhibit a second molecule of Cdc20<sup>9-13</sup>. Once all the  
62 chromosomes have attached correctly to the microtubules of the spindle through their  
63 kinetochores, the SAC is inactivated and Cdc20 is released to activate the APC/C against  
64 cyclin B1 and securin<sup>14,15</sup>, leading to the activation of separase and subsequently M-phase  
65 exit. The SAC ensures that sister chromatids will segregate to opposite spindle poles once  
66 the cohesion complexes are cleaved by separase.

67 The first mitotic division is highly unique as it is markedly longer than subsequent divisions  
68 in many species, including mouse<sup>16,17</sup>, Xenopus<sup>18,19</sup>, sea urchins and nematodes<sup>19</sup>. In mouse  
69 embryos the first mitosis lasts for 90-120 min, whereas the second lasts only 60-80 min<sup>16,17</sup>.  
70 The human first embryonic mitosis is also very long (approximately 2,5-3hrs<sup>20-24</sup>), and  
71 although there are no published data on the length of the second embryonic mitosis, some  
72 observations confirm that it tends to be markedly shorter (R. Milewski, J. Czerniecki, S.

73 Wołczyński, unpublished data). By comparison, in somatic cells the length of M-phase varies  
74 between 30 and 60 min, depending on the cell type and on the length of the SAC-regulated  
75 prometaphase, i.e. the period when the spindle and correct kinetochore-microtubule  
76 attachments are formed<sup>25-29</sup>.

77 One of the mechanisms that might prolong the first embryonic M-phase involves Emi2, an  
78 inhibitor of Cdc20<sup>30-32</sup>. The accumulation of Emi2 in metaphase II oocytes inhibits APC/C and  
79 thus maintains high levels of cyclin B1 and securin prior to fertilization<sup>33,34</sup>. Sperm  
80 penetration releases the oocyte from the Emi2-induced M-phase arrest by triggering  
81 phosphorylation of Emi2 by Ca<sup>2+</sup>/calmodulin dependent kinase II (CaMKII) and Plk1, which  
82 subsequently targets it for degradation<sup>30,35-37</sup>. Emi2 protein reappears in zygotes and it has  
83 been hypothesised that this contributes to the prolonged zygotic M-phase<sup>32,38</sup>. Alternatively,  
84 zygotic M-phase has also been proposed to be prolonged by a pool of stable cyclin A2 that  
85 inhibits efficient ubiquitination of cyclin B1 and securin by the APC/C<sup>39,40</sup>.

86 Here, we have investigated how the APC/C is regulated at the 1- to 2-cell transition in  
87 mouse embryos by assaying the degradation of cyclin A2 and cyclin B1. We find that, unlike  
88 in somatic cells, the APC/C does not appear to be activated at NEBD because we find cyclin  
89 A2 is stable in cells for over 30 min after NEBD, and cyclin B1 is stable for more than 45 min.  
90 We show that this delay in APC/C activation is most likely not caused by residual Emi2 but  
91 instead depends on Plk1 activity. Moreover, our experiments reveal that cyclin A2  
92 degradation is repressed by the SAC. Thus, we find that the prolonged first mammalian  
93 mitosis correlates with an unusual behaviour of the APC/C.

## 94 **Results**

### 95 **Spatiotemporal dynamics of cyclin A2 and cyclin B1 in mouse zygotes**

96 To determine how the very first embryonic M-phase is regulated, we assayed the  
97 spatiotemporal dynamics of cyclin A2 and B1. To this end, we injected zygotes or 2-cell  
98 embryos with synthetic mRNAs encoding either cyclin A2 tagged with YFP (cyclin A2-YFP), or  
99 cyclin B1 tagged with YFP or with Ruby (cyclin B1-YFP and cyclin B1-Ruby) and filmed their  
100 development through the first two mitotic divisions. We found that cyclin A2 was localized

101 in zygotic pronuclei during interphase, released into the cytoplasm during NEBD, degraded  
102 before the onset of anaphase, then resynthesized and imported into nuclei after the  
103 completion of division (Fig. 1a, **Supplementary Video S1**). In 2-cell embryos cyclin A2  
104 degradation started at NEBD, exactly as in somatic cells<sup>1,2</sup>, but in zygotes it was significantly  
105 delayed (**median of 39.0 min post NEBD, p<0.001**) and subsequently proceeded at a slow  
106 rate (Fig. 1a,c, Table 1). **The observation that cyclin A2 remained stably expressed at a high**  
107 **level for over 30 min after NEBD in zygotes indicated that activation of APC/C was delayed**  
108 **rather than partially activated. In the latter situation, cyclin A2 degradation would be**  
109 **initiated at the NEBD but proceed with slower kinetics.**

110 Assaying cyclin B1 showed that it was excluded from the nucleus for most of interphase and  
111 imported into the nucleus during prophase, approximately 30 min before NEBD. At NEBD  
112 cyclin B1 was released into the cytoplasm and bound the mitotic apparatus (Fig. 1b,  
113 **Supplementary Video S2**). We found that cyclin B1 was degraded at a similar rate during the  
114 first and second mitotic divisions (Fig. 1d), but, as with cyclin A2, the onset of cyclin B1  
115 degradation in the first mitotic division was significantly delayed in comparison to the  
116 second mitotic division (**medians of 48.0 and 18.0 min from NEBD, respectively**, p<0.001,  
117 Fig. 1b,d, Table 2). The delay in the degradation of cyclin A2 and cyclin B1 corresponded to  
118 the prolonged duration of the whole M-phase in zygotes when compared to 2-cell embryos  
119 (**medians of 111.0 and 57.0 min, respectively**, p<0.001, for cyclin A2-YFP embryos, and **96.0**  
120 **and 76.5 min**, p<0.001, for cyclin B1-Ruby embryos, Table 1,2). However, when we tested  
121 the correlation between the onset time of cyclin degradation and the duration of M-phase,  
122 we found that only the delay in cyclin B1 degradation, and not in cyclin A2 degradation,  
123 correlated with the length of M-phase (R=0.67, p<0.001). Taken together these results  
124 indicate that the prolonged duration of the first mitotic division might be caused by the  
125 delayed degradation **of cyclin B1**.

### 126 **Delayed degradation of cyclin A2 does not affect the timing of cyclin B1 degradation**

127 As late degradation of cyclin A2 did not seem to correlate with prolongation of the first  
128 embryonic M-phase, we directly addressed whether the high levels of cyclin A2 in zygotes

129 after NEBD might reduce the ability of the APC/C to ubiquitylate cyclin B1 and delay its  
130 degradation. To test this hypothesis, we examined the effect of over-expressing cyclin A2 on  
131 the rate of cyclin B1 degradation. To this end, zygotes were injected with mRNA encoding  
132 cyclin B1-Ruby and various concentrations (0.0-0.4  $\mu\text{g}/\mu\text{l}$ ) of mRNA encoding cyclin A2-YFP.  
133 **The increasing concentrations of mRNA translated into increasing amounts of cyclin A2**  
134 **protein as judged by an increase in fluorescence signal (Fig. 2a).** We found that  
135 overexpressing cyclin A2-YFP did not change the onset of cyclin B1-Ruby degradation (Fig.  
136 2a, Table 2). We next followed degradation of cyclin B1-Ruby and cyclin A2-YFP  
137 simultaneously in zygotes. This revealed that cyclin B1-Ruby started to be degraded on  
138 average **3 min** after cyclin A2 degradation, and at that time the level of cyclin A2 had only  
139 decreased on average by **0.7%** (Fig. 2b). These results indicated that the delay in cyclin B1  
140 degradation was not due to the late degradation of cyclin A2.

#### 141 **The SAC controls both cyclin B1 and cyclin A2 degradation**

142 In somatic cells a strong SAC signal does not prevent cyclin A2 degradation, although it slows  
143 it down<sup>41</sup>, but it does prevent cyclin B1 degradation<sup>8,14</sup>. Since degradation of both cyclin A2  
144 and B1 was delayed in the first embryonic M-phase, we wished to investigate whether the  
145 SAC was responsible for this. To test this hypothesis, we determined the effect of inhibiting  
146 the Mps1 kinase, **an essential activator** of the SAC<sup>42,43</sup>, on the dynamics of cyclin A2 and  
147 cyclin B1 degradation. We injected zygotes with cyclin A2-YFP or cyclin B1-Ruby and assayed  
148 their development in the presence of reversine, an Mps1 inhibitor<sup>42</sup>. We found that  
149 inhibiting the SAC shortened the period between NEBD and the onset of cyclin B1-Ruby  
150 degradation (**to the median of 39 min**,  $p < 0.05$ , Fig. 3a, Table 2). Similarly, reversine  
151 accelerated the onset of securin-GFP degradation (from **the median of 36 min to 24 min**,  
152  $p < 0.001$ ; Supplementary Fig. S1a, Supplementary Table S1). Unlike in somatic cells, ablating  
153 the SAC in zygotes advanced the timing of cyclin A2-YFP degradation (**to the median of 3**  
154 **min**,  $p < 0.001$ , Fig. 3b). We concluded that the SAC affects the timing of the cyclin B1 and A2  
155 degradation and thus might be partially responsible for the prolonged first mouse  
156 embryonic M-phase. Inactivation of the SAC during the first division did not, however,  
157 shorten the time between NEBD and the onset of cyclin B1 or cyclin A2 degradation to the

158 length comparable with the period observed in the subsequent division ( $p < 0.001$  and  $p < 0.05$   
159 respectively, Table 1,2). This indicated that there was an additional mechanism regulating  
160 the onset of cyclin B1 and A2 degradation and, in consequence, the length of the first M-  
161 phase.

## 162 **Emi2 is not involved in regulation of the first embryonic M-phase**

163 The first mechanism we considered was APC/C inhibition by maternal Emi2, which is  
164 responsible for maintaining oocytes in metaphase II. It had previously been suggested that  
165 prolongation of the first embryonic M-phase was caused by the persistence of Emi2 that is  
166 resynthesized in zygotes after its degradation triggered by fertilisation<sup>32</sup>. To address  
167 whether Emi2 was responsible for the delay in cyclin degradation and the prolonged zygotic  
168 M-phase, we depleted Emi2 with specific morpholinos (Emi2 MO), which had been shown to  
169 block the translation of Emi2 mRNA<sup>33</sup>. Since Emi2 is required to inhibit the APC/C and  
170 maintain oocytes in metaphase II, we assayed the effectiveness of the Emi2 MO to deplete  
171 Emi2 by co-injecting Emi2 MO with cyclin B1-YFP into metaphase II oocytes and measured  
172 the level of cyclin B1-YFP fluorescence and oocyte activation. We found that 75% of oocytes  
173 injected with Emi2 MO (33/44), but only 9% (2/22) oocytes injected with a control MO (Emi2  
174 MO with 5 mismatched pairs of nucleotides, Emi2 5-MP MO) underwent activation within  
175 24 hrs of injection (Supplementary Fig. S2a). Moreover, there was an abrupt decrease in  
176 cyclin B1-YFP 12 hrs after microinjection of Emi2 MO, whereas in oocytes co-injected with  
177 Emi2 5-MP MO cyclin B1 remained stable (Supplementary Fig. S2b). These results  
178 demonstrated that we could efficiently deplete Emi2 through this approach. We injected  
179 Emi2 MO into very early zygotes, 2h post fertilization and well before pronuclei formation,  
180 at the time, when Emi2 protein is completely degraded<sup>33</sup>. This ensured that the morpholinos  
181 were injected in time to prevent re-synthesis of Emi2 after its degradation at meiotic  
182 exit<sup>32,33</sup>. We found that zygotes injected with Emi2 MO behaved exactly as the control-  
183 injected zygotes with no shortening of the M-phase and no difference in the timing of cyclin  
184 B1 degradation (medians of 40 and 45 min, respectively,  $p > 0.05$ , Fig. 4a).

185 As a further test of the potential role of Emi2 in prolonging M-phase, we depleted Emi2 by  
186 siRNA. To this end, we injected GV stage oocytes with mRNA encoding securin-GFP together  
187 with siRNA specific for Emi2 or control siRNA, allowed them to mature in vitro until  
188 metaphase II, then activated them parthenogenetically and assayed them through the first  
189 embryonic division. Emi2 depletion did not accelerate the onset of securin degradation  
190 (Supplementary Fig. S3a,b), even though the efficiency of Emi2 siRNA was confirmed by its  
191 ability to release metaphase II arrest in injected oocytes (Supplementary Fig. S3c). Taken  
192 together, these results show that Emi2 is **unlikely to be** responsible for the delay in  
193 degradation of APC/C substrates during the first embryonic M-phase.

#### 194 **Plk1 controls both cyclin B1 and cyclin A2 degradation in a SAC-independent manner**

195 We then tested the possibility that Plk1 might be responsible for the delay in cyclin  
196 degradation because it **is important for the full activation** of the APC/C<sup>44-46</sup>. Moreover, Plk1  
197 is essential for the completion of the first embryonic cell cycle in the mouse<sup>47,48</sup>. To examine  
198 whether Plk1 might be involved in regulating cyclin B1 and A2 turnover in the first M-phase  
199 in mouse, we injected zygotes with mRNAs encoding wt Plk1 and cyclins (A2 or B1) and then  
200 assayed their development. We found that over-expression of wt Plk1-YFP shortened the  
201 period between NEBD and the onset of cyclin B1-Ruby degradation to the length typical for  
202 the second M-phase (**to a median of 28.5 min**,  $p < 0.001$  when compared to the first M-phase  
203 and  $p > 0.05$  when compared to the second M-phase; Fig. 4b, Table 2). The duration of the  
204 whole M-phase was also shortened accordingly (**to a median of 78.0 min**,  $p < 0.001$  when  
205 compared to the first M-phase and  $p > 0.05$  when compared to the second M-phase, Table  
206 2). Over-expression of an inactive, kinase dead Plk1 (kd Plk1-YFP) did not affect the  
207 degradation of cyclin B1 (Fig. 4b, Table 2), indicating that the observed acceleration of cyclin  
208 B1 degradation required Plk1 activity. Over-expression of wt Plk1-TagRFP also advanced the  
209 onset of securin degradation (**to a median of 27.0 min**,  $p < 0.05$ ; Supplementary Fig. S1b,  
210 Supplementary Table S1). Remarkably, we found that although Plk1 is not required for cyclin  
211 A2 to be degraded in somatic cells<sup>49</sup>, over-expressing Plk1-TagRFP significantly accelerated  
212 the onset of cyclin A2-YFP degradation in zygotes (**to a median of 15 min** post NEBD,  $p < 0.05$ )  
213 (Fig. 4c, Table 1), although it still occurred on average later than in 2-cell embryos ( $p < 0.05$ ,



214 Table 1).

215 As a further test of whether Plk1 was involved in regulating the first embryonic M-phase, we  
216 inhibited Plk1 with the small molecule inhibitor BI2536<sup>49</sup> and assessed zygotic division by  
217 time-lapse microscopy. This revealed that BI2536 significantly delayed the onset of cyclin B1  
218 degradation (to a median of 93.0 min post NEBD,  $p < 0.05$ ; Fig. 4b, Table 2). Although we  
219 observed some gradual decrease of cyclin B1 in zygotes treated with BI2536, it was never  
220 sufficient to induce anaphase (Supplementary Fig. S4a). The inhibition of Plk1 also  
221 prevented the degradation of cyclin A2, which persisted at a high level for over 2h post  
222 NEBD (Fig. 4c, Table 1). We found that inhibiting Plk1 activity did not interfere with the  
223 formation of a bi-polar spindle, in agreement with a recent report<sup>48</sup>. However, we found  
224 that the spindle gradually deteriorated during the prolonged M-phase arrest; specifically the  
225 spindle poles became less focused over time and displayed increased numbers of astral  
226 microtubules, and in some cases chromosomes were displaced from the metaphase plate  
227 (Supplementary Fig. S4a).

228 To address whether Plk1 altered the length of the first M-phase by altering SAC activity, we  
229 asked whether reversine could override the zygotic M-phase arrest induced by Plk1  
230 inhibition. We found that neither reversine, nor injection of mRNA encoding a dominant  
231 negative Mad2 (dn Mad2), was able to release zygotes from a BI2536-induced M-phase  
232 arrest (Supplementary Fig. S4b). Moreover, reversine was not able to counteract the  
233 BI2536-induced delay in cyclin B1 degradation (Fig. 4d, Table 2).

234 Finally, since our results indicated that Plk1 activity might be limiting in the first M-phase of  
235 the mouse embryo, we investigated whether the amount of active Plk1 (i.e. Plk1  
236 phosphorylated at Thr210) differs between M-phase zygotes and 2-cell embryos.  
237 Quantitative analysis of the intensity of phospho-Plk1 (pPlk1) immunostaining indicated that  
238 active Plk1 was slightly more abundant in M-phase 2-cell embryos than in M-phase zygotes,  
239 although the difference did not reach statistical significance ( $p = 0.058$ ; Supplementary Fig.  
240 S5a,b). Interestingly, we observed that there was a subtle, but potentially important,  
241 difference in pPlk1 localization in 1- and 2-cell stage embryos. In both the first and the

242 second M-phase pPlk1 localized to the spindle poles and chromosomes; however, in 2-cell  
243 embryos it strongly accumulated on kinetochores, whereas in zygotes its chromosomal  
244 distribution was more diffuse (Supplementary Figure S5c).

245 Taken together these results indicate that the degradation of cyclins B1 and A2, and in  
246 consequence the prolonged first M-phase, is regulated by a Plk1-dependent mechanism. We  
247 propose that a difference in the localization of active Plk1 might potentially be involved in  
248 prolongation of the first embryonic M-phase in the mouse.

## 249 Discussion

250 The first embryonic mitosis in a number of species is strikingly longer than the subsequent  
251 embryonic mitoses and mitosis in somatic cells<sup>19,50</sup>. Indeed, the first zygotic M-phase is  
252 unique because during this period two sets of chromosomes, enclosed in separate nuclei,  
253 need to form a single metaphase plate. This process is more complicated than its equivalent  
254 in a typical mononuclear somatic cell, and therefore most likely more time is required to  
255 ensure appropriate chromosome-spindle connections. It appears plausible to us that this is  
256 the biological purpose of the prolonged first zygotic M-phase, and particularly the period  
257 between NEBD and cyclin B1 degradation.

258 Here, we have uncovered atypical APC/C behaviour in the first mitotic division that appears  
259 to be responsible for this extended M-phase. Our analysis of the spatiotemporal dynamics  
260 of cyclin A2 and cyclin B1 indicates that length of the first M-phase is likely a consequence of  
261 delayed APC/C activation. We find that cyclin A2 starts to be degraded in zygotes over 30  
262 min after NEBD, in striking contrast to 2-cell embryos or somatic cells where cyclin A2 begins  
263 to be degraded at NEBD. The degradation of cyclin B1 and securin in zygotes is also  
264 significantly delayed in comparison to mitosis in 2-cell embryos, and to somatic cells<sup>8,14</sup>.  
265 Although it has been hypothesized that the stable pool of cyclin A2 is responsible for the  
266 prolonged M-phase in zygotes<sup>39,40</sup>, our results do not support this idea because we find that  
267 cyclin B1 starts to be degraded when the levels of cyclin A2 are still very high. Furthermore,  
268 overexpressing cyclin A2 does not delay the onset of cyclin B1 degradation. However, in

269 accordance with published data<sup>1,2,51</sup> we observed that overexpression of cyclin A2 disturbs  
270 progression of anaphase and cytokinesis.

271 Our experiments provide evidence that the SAC regulates APC/C activity towards cyclin A2  
272 in the first M-phase in mouse because inhibiting the SAC both advances and accelerates the  
273 degradation of cyclin A2 (and B1). However, our results also indicate that SAC activity is not  
274 solely responsible for the prolongation of the zygotic M-phase since inhibiting the SAC  
275 accelerated the onset of cyclin degradation by only approximately 10-20 min. This agrees  
276 with earlier work showing that SAC proteins, such as Mad2 leave, the kinetochores in  
277 zygotes within approximately 20 min of NEBD<sup>17</sup>, and a similar delay in cyclin B1 degradation  
278 is caused by the SAC in somatic cells<sup>27,29</sup>. Thus, there must be another mechanism involved  
279 in the delay in degradation of cyclins A2 and B1, and as a result, the prolongation of zygotic  
280 M-phase.

281 Our evidence implicates Plk1 as the additional factor responsible for the first mitotic delay.  
282 Plk1 activity appears to be a limiting factor because overexpression of Plk1 accelerates the  
283 onset of cyclin A2 and B1 degradation, even though in somatic cells Plk1 activity is not  
284 required for the APC/C to target cyclin A2 at NEBD<sup>49,52</sup>. Moreover, Plk1 overexpression  
285 shortens the period between NEBD and the onset of cyclin B1-Ruby degradation to the  
286 length typical for the second embryonic mitosis. We show that Plk1 does not act exclusively  
287 through the SAC, since ablation of the SAC does not rescue the delay caused by Plk1  
288 inhibition. Plk1 is also unlikely to act through Emi2 since the injection of Emi2-specific  
289 morpholinos or siRNAs did not accelerate cyclin B1 or securin degradation during the first  
290 embryonic division. However, we cannot completely exclude the possibility that in zygotic  
291 M-phase even a very small amount of Emi2 that potentially may remain in the cell after MO-  
292 or siRNA-induced depletion is sufficient to inhibit APC/C activity. Indeed, the role of Emi2 in  
293 the first mitotic divisions is currently debated in *Xenopus* embryos<sup>34,53</sup>. Instead, our  
294 evidence would be congruent with a role for Plk1 in activating the APC/C in embryonic  
295 divisions through direct phosphorylation of the APC/C complex<sup>45,46,52,54</sup>.

296

297 If Plk1 is indeed a limiting factor in the zygotic M-phase, then it should either be expressed  
298 at lower levels in zygotes, or be differently regulated. Analysis of transcriptomic data  
299 available in the DBTMEE database (RNA-seq Ver2\_FPKM collection, <http://dbtmee.hgc.jp/>)<sup>55</sup>  
300 indicates that Plk1 mRNA expression is higher in zygotes than in 2-cell embryos, but we find  
301 that the amount of active Plk1 is comparable – with a tendency to be lower - between M-  
302 phase zygotes and 2-cell embryos. Comparing the expression of Plk1 activators / inhibitors  
303 also does not reveal a clear difference between these two stages: some transcripts are more  
304 abundant in zygotes, others in 2-cell embryos. Alternatively, the difference between the  
305 mode of Plk1 action in the first and the second embryonic divisions may relate to the  
306 distribution of active Plk1: in contrast to 2-cell embryos, in zygotes, pPlk1 does not  
307 accumulate very effectively on kinetochores.

308 Taken together, we conclude that the APC/C has reduced activity in the first embryonic  
309 division that extends the first M-phase. As a consequence we find that cyclin A2 degradation  
310 in the first mitosis is atypical, resembling the way in which cyclin B1 is controlled in somatic  
311 cells, because its degradation is regulated by both SAC and Plk1 activities. Our observations  
312 shed new light on the molecular machinery controlling the unusual length of the first  
313 embryonic division

## 314 **Methods**

### 315 **Embryo collection and culture**

316 All experimental procedures applied to animals were approved by the Home Office (UK) or  
317 by the Local Ethical Committee no. 1 (Warsaw, Poland), and were performed in compliance  
318 with the national regulations. Mouse F1 (C57Bl6 x CBA) females were superovulated by an  
319 intraperitoneal injection of 10 IU of pregnant mare serum gonadotrophin (PMSG, Intervet)  
320 followed 48 hrs later by 10 IU of human chorionic gonadotrophin (hCG, Intervet) and mating  
321 with F1 males. Zygotes and 2-cell embryos were recovered from oviducts into M2 medium  
322 16-20 hrs and 44 hrs after hCG injection, respectively. MII oocytes were recovered 15 hrs  
323 post hCG injection from oviducts of unmated females into M2 medium. GV oocytes were

324 recovered from ovaries 48 hrs after the PMSG injection into M2 medium supplemented with  
325 150 µg/ml dibutyryl cyclic AMP (dbcAMP, Sigma-Aldrich).

### 326 **Microinjections and live imaging of embryos**

327 Constructs encoding cyclin B1 tagged with YFP or Ruby (cyclin B1-YFP, cyclin B1-Ruby), cyclin  
328 A2 tagged with YFP (cyclin A2-YFP), Plk1 tagged with YFP or TagRFP (wt Plk1-YFP, wt Plk1-  
329 TagRFP), kinase dead version of Plk1 tagged with YFP (kd Plk1-YFP), dominant negative  
330 version of Mad2 (dn Mad2) and securin tagged with GFP (securin-GFP) were cloned into  
331 pBluescript RN3P vector and mRNA was synthesized from the T3 promotor using mMessage  
332 mMachinE T3 kit (Ambion), as described previously<sup>56</sup>. A construct encoding histone 2B  
333 tagged with RFP (H2B-RFP) was cloned into pGEMHE vector and synthesized from the T7  
334 promotor using mMessage mMachinE T7 kit (Ambion). mRNAs (needle concentration 0.025  
335 µg/µl for H2B-RFP, 0.07 µg/µl for cyclin B1-Ruby, 0.07 µg/µl for cyclin A2-YFP, 0.2 µg/µl for  
336 cyclin B1-YFP, wt Plk1-YFP and kd Plk1-YFP, 0.35 µg/µl for securin-GFP, 0.7 µg/µl for Plk1-  
337 TagRFP, 0.8 µg/µl dn Mad2) were injected into a zygote or one blastomere of a 2-cell stage  
338 embryo and injected embryos were subsequently cultured in KSOM (Speciality Media,  
339 Millipore) for approximately 6 hrs to allow for sufficient protein expression. In some  
340 experiments oocytes or embryos were injected with 25µM siRNA (Sigma-Aldrich) or 2mM  
341 morpholino<sup>33</sup> (Gene Tools LLC) specific to Emi2 and with appropriate controls  
342 (Supplementary Table S2). Emi2 MO was injected into early zygotes (recovered 16 hrs post  
343 hCG) together with cyclin B1-YFP, which then were cultured for approximately 8 hrs in  
344 KSOM. Emi2 siRNA was injected with securin-GFP into GV oocytes that were afterwards  
345 allowed to mature for 16 hrs and subsequently were activated parthenogenetically by  
346 incubation in 8% ethanol for 8 min and cultured for 8 hrs in KSOM. Zygotes,  
347 parthenogenotes or 2-cell embryos were transferred into M2 medium and imaged in 11-13  
348 planes (5-6 µm apart) every 3-15 min for 12 hrs over the transition from 1- to 2-cell stage or  
349 2- to 4-cell stage. In some experiments M2 was supplemented with 500 nM reversine  
350 (Sigma-Aldrich) or 100 nM BI2536 (Axon Medchem). Imaging was performed on a 3i  
351 Intelligent Imaging Solutions spinning-disc confocal microscope, Zeiss Axiovert fluorescence

352 microscope or Deltavision fluorescence microscope, all equipped with environmental  
353 chambers maintaining temperature of 37.5°C.

#### 354 **Immunostaining**

355 Embryos were fixed in 4% PFA (30 min, RT), permeabilised with 0.5% Triton-X100 (30 min,  
356 RT) and blocked with 3% BSA. Plk1 phosphorylated at Thr210 was labeled with a polyclonal  
357 rabbit antibody (ThermoFisher Scientific; dilution 1:100 in 3% BSA, overnight, 4 °C) and  
358 cyclinA2 - with a polyclonal rabbit antibody (Santa Cruz; dilution 1:50 in 3% BSA, overnight,  
359 4 °C), both followed by a secondary anti-rabbit antibody conjugated with Alexa 633  
360 (Molecular Probes, ThermoFisher Scientific; dilution 1:200 in 3% BSA, 1.5h, RT).

361 Microtubules were stained with mouse anti-tubulin  $\beta$  antibody labeled with FITC (Sigma-  
362 Aldrich; dilution 1:50 in 3% BSA, 1.5h, RT or overnight, 4°C) DNA was stained with Hoechst  
363 33342 dye (Molecular Probes, ThermoFisher Scientific; 100ng/ $\mu$ l in PBS, 30 min, RT or  
364 overnight, 4°C), propidium iodide (Sigma-Aldrich; 3  $\mu$ g/ml in PBS, 30 min, RT) or  
365 chromomycin A3 (Sigma-Aldrich; 10  $\mu$ g/ml, 30 min, RT or overnight, 4°C). In case of  
366 phospho-Plk1 detection, a PhosStop solution (Roche) was added to all stages of  
367 immunostaining to inhibit phosphatases.

#### 368 **Statistical analysis**

369 In order to quantify cyclin B1 or cyclin A2 levels in embryos, projections (sums of all slices)  
370 were prepared for all imaged embryos and mean fluorescence intensity was measured for  
371 each projection over the time of recording. The intensity values were then standardized  
372 with the fluorescence intensity at the NEBD. Polynomial curves were fitted to the data and  
373 the onset of cyclin or securin degradation was established as the first time-point after NEBD  
374 when the fluorescence decrease between two subsequent measurements was at least 0.01.  
375 Statistical analyses of results were performed using Student's t-test, chi-squared test,  
376 Spearman's rank-order correlation and Kruskal-Wallis test with a post-hoc multiple  
377 comparison of mean ranks test.

378

379 **References**

- 380 1. den Elzen, N. & Pines, J. Cyclin A is destroyed in prometaphase and can delay  
381 chromosome alignment and anaphase. *J. Cell Biol.* **153**, 121-136 (2001).
- 382 2. Geley, S. *et al.* Anaphase-promoting complex/cyclosome-dependent proteolysis of  
383 human cyclin A starts at the beginning of mitosis and is not subject to the spindle  
384 assembly checkpoint. *J. Cell Biol.* **153**, 137-148 (2001).
- 385 3. Musacchio, A. & Salmon, E. D. The spindle-assembly checkpoint in space and time. *Nat.*  
386 *Rev. Mol. Cell Biol.* **8**, 379-393 (2007).
- 387 4. Lara-Gonzalez, P., Westhorpe, F. G. & Taylor, S. S. The spindle assembly checkpoint. *Curr.*  
388 *Biol.* **22**, R966-80 (2012).
- 389 5. Di Fiore, B. & Pines, J. How cyclin A destruction escapes the spindle assembly  
390 checkpoint. *J. Cell Biol.* **190**, 501-509 (2010).
- 391 6. Wolthuis, R. *et al.* Cdc20 and Cks direct the spindle checkpoint-independent destruction  
392 of cyclin A. *Mol. Cell* **30**, 290-302 (2008).
- 393 7. Di Fiore, B. *et al.* The ABBA motif binds APC/C activators and is shared by APC/C  
394 substrates and regulators. *Dev. Cell* **32**, 358-372 (2015).
- 395 8. Izawa, D. & Pines, J. How APC/C-Cdc20 changes its substrate specificity in mitosis. *Nat.*  
396 *Cell Biol.* **13**, 223-233 (2011).
- 397 9. Sudakin, V., Chan, G. K. & Yen, T. J. Checkpoint inhibition of the APC/C in HeLa cells is  
398 mediated by a complex of BUBR1, BUB3, CDC20, and MAD2. *J. Cell Biol.* **154**, 925-936  
399 (2001).
- 400 10. Chao, W. C., Kulkarni, K., Zhang, Z., Kong, E. H. & Barford, D. Structure of the mitotic  
401 checkpoint complex. *Nature* **484**, 208-213 (2012).
- 402 11. Izawa, D. & Pines, J. The mitotic checkpoint complex binds a second CDC20 to inhibit  
403 active APC/C. *Nature* **517**, 631-634 (2015).
- 404 12. Alfieri, C. *et al.* Molecular basis of APC/C regulation by the spindle assembly checkpoint.  
405 *Nature* **536**, 431-436 (2016).

- 406 13. Yamaguchi, M. *et al.* Cryo-EM of mitotic checkpoint complex-bound APC/C reveals  
407 reciprocal and conformational regulation of ubiquitin ligation. *Mol. Cell* **63**, 593-607  
408 (2016).
- 409 14. Clute, P. & Pines, J. Temporal and spatial control of cyclin B1 destruction in metaphase.  
410 *Nat. Cell Biol.* **1**, 82–87 (1999).
- 411 15. Hagting, A. *et al.* Human securin proteolysis is controlled by the spindle checkpoint and  
412 reveals when the APC/C switches from activation by Cdc20 to Cdh1. *J. Cell Biol.* **157**,  
413 1125-37 (2002).
- 414 16. Maciejewska, Z., Polanski, Z., Kisiel, K., Kubiak, J. Z. & Ciemerych, M. A. Spindle assembly  
415 checkpoint-related failure perturbs early embryonic divisions and reduces reproductive  
416 performance of LT/Sv mice. *Reproduction* **137**, 931–942 (2009).
- 417 17. Sikora-Polaczek, M., Hupalowska, A., Polanski, Z., Kubiak, J. Z. & Ciemerych, M. A. The  
418 first mitosis of the mouse embryo is prolonged by transitional metaphase arrest. *Biol.*  
419 *Reprod.* **74**, 734–743 (2006).
- 420 18. Chesnel, F., Vignaux, F., Richard-Parpaillon, L., Huguet, A. & Kubiak, J. Z. Differences in  
421 regulation of the first two M-phases in *Xenopus laevis* embryo cell-free extracts. *Dev.*  
422 *Biol.* **285**, 358–375 (2005).
- 423 19. Kubiak, J. Z. *et al.* Temporal regulation of the first mitosis in *Xenopus* and mouse  
424 embryos. *Mol. Cell Endocrinol.* **282**, 63-69 (2008).
- 425 20. Chamayou, S. *et al.* The use of morphokinetic parameters to select all embryos with full  
426 capacity to implant. *J. Assist. Reprod. Genet.* **30**, 703-710 (2013).
- 427 21. Desai, N. *et al.* Analysis of embryo morphokinetics, multinucleation and cleavage  
428 anomalies using continuous time-lapse monitoring in blastocyst transfer cycles. *Reprod.*  
429 *Biol. Endocrinol.* **12**, 54; 10.1186/1477-7827-12-54 (2014).
- 430 22. Chawla, M. *et al.* Morphokinetic analysis of cleavage stage embryos and its relationship  
431 to aneuploidy in a retrospective time-lapse imaging study. *J. Assist. Reprod. Genet.* **32**,  
432 69-75 (2015).
- 433 23. Liu, Y., Chapple, V., Feenan, K., Roberts, P. & Matson P. Time-lapse videography of  
434 human embryos: Using pronuclear fading rather than insemination in IVF and ICSI cycles



- 435 removes inconsistencies in time to reach early cleavage milestones. *Reprod. Biol.* **15**,  
436 122-125 (2015).
- 437 24. Storr, A. *et al.* Morphokinetic parameters using time-lapse technology and day 5 embryo  
438 quality: a prospective cohort study. *J. Assist. Reprod. Genet.* **32**, 1151-1160 (2015).
- 439 25. Rieder, C. L., Schultz, A., Cole, R. & Sluder, G. Anaphase onset in vertebrate somatic cells  
440 is controlled by a checkpoint that monitors sister kinetochore attachment to the spindle.  
441 *J. Cell Biol.* **127**, 1301–1310 (1994).
- 442 26. Gorbsky, G. J., Chen, R. H. & Murray, A. W. Microinjection of antibody to Mad2 protein  
443 into mammalian cells in mitosis induces premature anaphase. *J. Cell Biol.* **141**, 1193–  
444 1205 (1998).
- 445 27. Howell, B. J., Hoffman, D. B., Fang, G., Murray, A. W. & Salmon, E. D. Visualization of  
446 Mad2 dynamics at kinetochores, along spindle fibers, and at spindle poles in living cells.  
447 *J. Cell Biol.* **150**, 1233–1250 (2000).
- 448 28. Jones, J. T., Myers, J. W., Ferrell, J. E. & Meyer, T. Probing the precision of the mitotic  
449 clock with a live-cell fluorescent biosensor. *Nat. Biotech.* **22**, 306–312 (2004).
- 450 29. Meraldi, P., Draviam, V. M. & Sorger, P. K. Timing and checkpoints in the regulation of  
451 mitotic progression. *Dev. Cell* **7**, 45–60 (2004).
- 452 30. Rauh, N. R., Schmidt, A., Bormann, J., Nigg, E. A. & Mayer, T. U. Calcium triggers exit  
453 from meiosis II by targeting the APC/C inhibitor XErp1 for degradation. *Nature* **437**,  
454 1048–1052 (2005).
- 455 31. Tung, J. J. *et al.* A role for the anaphase-promoting complex inhibitor Emi2/XErp1, a  
456 homolog of early mitotic inhibitor 1, in cytostatic factor arrest of *Xenopus* eggs. *Proc.*  
457 *Natl. Acad. Sci. U. S. A.* **102**, 4318-4323 (2005).
- 458 32. Shoji, S. *et al.* Mammalian Emi2 mediates cytostatic arrest and transduces the signal for  
459 meiotic exit via Cdc20. *EMBO J.* **25**, 834–845 (2006).
- 460 33. Madgwick, S., Hansen, D. V., Levasseur, M., Jackson, P. K. & Jones, K. T. Mouse Emi2 is  
461 required to enter meiosis II by reestablishing cyclin B1 during interkinesis. *J. Cell Biol.*  
462 **174**, 791–801 (2006).
- 463 34. Tischer, T., Hörmanseder, E. & Mayer, T. U. The APC/C inhibitor XErp1/Emi2 is essential  
464 for *Xenopus* early embryonic divisions. *Science* **338**, 520–524 (2012).

- 465 35. Liu, J. & Maller, J. L. Calcium elevation at fertilization coordinates phosphorylation of  
466 XErp1/Emi2 by Plx1 and CaMK II to release metaphase arrest by cytostatic factor. *Curr.*  
467 *Biol.* **15**, 1458–1468 (2005).
- 468 36. Schmidt, A. *et al.* Xenopus polo-like kinase Plx1 regulates XErp1, a novel inhibitor of  
469 APC/C activity. *Genes Dev.* **19**, 502–513 (2005).
- 470 37. Hansen, D. V., Tung, J. J. & Jackson, P. K. CaMKII and polo-like kinase 1 sequentially  
471 phosphorylate the cytostatic factor Emi2/XErp1 to trigger its destruction and meiotic  
472 exit. *Proc Natl. Acad. Sci. U.S.A.* **103**, 608–613 (2006).
- 473 38. Kubiak, J. Z., Ciemerych, M. A., Hupalowska, A., Sikora-Polaczek, M. & Polanski, Z. On the  
474 transition from the meiotic to mitotic cell cycle during early mouse development. *Int. J.*  
475 *Dev. Biol.* **52**, 201–217 (2008).
- 476 39. Winston, N. *et al.* Early development of mouse embryos null mutant for the cyclin A2  
477 gene occurs in the absence of maternally derived cyclin A2 gene products. *Dev. Biol.* **223**,  
478 139–153 (2000).
- 479 40. Kubiak, J. Z. & Ciemerych, M. A. Cell cycle regulation in early mouse embryos. *Novartis*  
480 *Found. Symp.* **237**, 79-89 (2001).
- 481 41. Collin, P., Nashchekina, O., Walker, R. & Pines, J. The spindle assembly checkpoint works  
482 like a rheostat rather than a toggle switch. *Nat. Cell Biol.* **15**, 1378-1385 (2013).
- 483 42. Santaguida, S., Tighe, A., D'Alise, A. M., Taylor, S. S. & Musacchio, A. Dissecting the role  
484 of MPS1 in chromosome biorientation and the spindle checkpoint through the small  
485 molecule inhibitor reversine. *J. Cell Biol.* **190**, 73–87 (2010).
- 486 43. Tipton, A. R. *et al.* Monopolar spindle 1 (MPS1) kinase promotes production of closed  
487 MAD2 (C-MAD2) conformer and assembly of the mitotic checkpoint complex. *J. Biol.*  
488 *Chem.* **288**, 35149–35158 (2013).
- 489 44. Petronczki, M., Lénárt, P. & Peters, J. M. Polo on the rise-from mitotic entry to  
490 cytokinesis with Plk1. *Dev. Cell* **14**, 646-659 (2008).
- 491 45. Fujimitsu, K., Grimaldi, M. & Yamano, H. Cyclin-dependent kinase 1-dependent  
492 activation of APC/C ubiquitin ligase. *Science* **352**, 1121-1214 (2016).
- 493 46. Zhang, S. *et al.* Molecular mechanism of APC/C activation by mitotic phosphorylation.  
494 *Nature* **533**, 260-264 (2016).

- 495 47. Baran, V., Solc, P., Kovarikova, V., Rehak, P. & Sutovsky, P. Polo-like kinase 1 is essential  
496 for the first mitotic division in the mouse embryo. *Mol. Reprod. Dev.* **80**, 522–534 (2013).
- 497 48. Baran, V., Brzakova, A., Rehak, P., Kovarikova, V. & Solc, P. PLK1 regulates spindle  
498 formation kinetics and APC/C activation in mouse zygote. *Zygote* **15**, 1-8 (2015).
- 499 49. Lénárt, P. *et al.* The small-molecule inhibitor BI 2536 reveals novel insights into mitotic  
500 roles of polo-like kinase 1. *Curr. Biol.* **17**, 304-315 (2007).
- 501 50. Hörmanseder, E., Tischler, T. & Mayer, T. U. Modulation of cell cycle control during  
502 oocyte-to-embryo transitions. *EMBO J.* **32**, 2191-2203 (2013).
- 503 51. Touati, S.A. *et al.* Cyclin A2 is required for sister chromatid segregation, but not separase  
504 control, in mouse oocyte meiosis. *Cell Rep.* **2**, 1077-1087 (2012)
- 505 52. Kraft, C. *et al.* Mitotic regulation of the human anaphase-promoting complex by  
506 phosphorylation. *EMBO J.* **22**, 6598-6609 (2003).
- 507 53. Liu, J., Grimison, B., Lewellyn, A. L. & Maller, J. L. The anaphase-promoting  
508 complex/cyclosome inhibitor Emi2 is essential for meiotic but not mitotic cell cycles. *J.*  
509 *Biol. Chem.* **281**, 34736–34741 (2006).
- 510 54. Golan, A., Yudkovsky, Y. & Hershko, A. The cyclin-ubiquitin ligase activity of  
511 cyclosome/APC is jointly activated by protein kinases Cdk1-cyclin B and Plk. *J. Biol. Chem.*  
512 **277**, 15552-15557 (2002).
- 513 55. Park, S.J., Shirahige, K., Ohsumi, M. & Nakai, K. DBTMEE: a database of transcriptome in  
514 mouse early embryos. *Nucleic Acids Res.* **43**, D771-776 (2015).
- 515 56. Zernicka-Goetz, M. *et al.* Following cell fate in the living mouse embryo. *Development*  
516 **124**, 1133–1137 (1997).

517

## 518 **Acknowledgements**

519 We would like to thank Aleksander Chlebowski and Drs Takao Ishikawa and Robert Milewski  
520 for their valuable assistance. We are grateful to the Wellcome Trust, which supported this  
521 work. AA was a beneficiary of the Kolumb programme and the subsequent Kolumb  
522 supporting grant of the Foundation for Polish Science. MZG is supported by the Wellcome  
523 Trust.

524 **Author contributions**

525 A.A. designed and conducted the experiments and wrote the manuscript. B.S. conducted  
526 the experiments and reviewed the manuscript. M.Z.-G. and J.P. designed the experiments  
527 and wrote the manuscript.

528 **Competing financial interests**

529 The authors declare no competing financial interests.

530

531

532 **Figure legends**

533 **Figure 1**

534 **Spatiotemporal dynamics of cyclins A2 and B1 in mouse embryos**

535 (a) Spatiotemporal dynamics of cyclin A2-YFP in dividing zygotes. Selected images from a  
536 time-lapse recording, time shown in hours and minutes counted from the timepoint of  
537 nuclear envelope breakdown (NEBD). (b) Spatiotemporal dynamics of cyclin B1-YFP in  
538 dividing zygotes. Selected images from a time-lapse recording, time shown in hours and  
539 minutes counted from the timepoint of NEBD. (c) Quantification of cyclin A2-YFP  
540 degradation in 1- and 2-cell embryos, averaged from 30 and 37 embryos respectively. (d)  
541 Quantification of cyclin B1-Ruby degradation in 1- and 2-cell embryos, averaged from 55 and  
542 31 embryos respectively. Scale bars in (a) and (b) are 20  $\mu\text{m}$ . Plots in (c) and (d) show mean  
543 values +/- standard deviation.

544 **Figure 2**

545 **Role of cyclin A2 in regulation of cyclin B1 degradation**

546 (a) Quantification of cyclin B1-Ruby degradation in zygotes injected with increasing  
547 concentrations (0, 0.07  $\mu\text{g}/\mu\text{l}$ , 0.2  $\mu\text{g}/\mu\text{l}$ , 0.4  $\mu\text{g}/\mu\text{l}$ ) of cyclin A2-YFP mRNA, averaged from  
548 55, 41, 12 and 10 embryos respectively. Plots show mean values +/- standard deviation.

549 Images show representative zygotes injected with increasing concentrations of cyclin A2-YFP  
550 mRNA and the same concentration of cyclin B1 mRNA. Overexpression of cyclin A2 was  
551 confirmed by an immunostaining (the bottom panel). Scale bar is 100  $\mu\text{m}$ . (b) Quantification  
552 of cyclin B1-Ruby and cyclin A2-YFP degradation in a single representative zygote.

### 553 **Figure 3**

#### 554 **Role of SAC in regulation of cyclin A2 and B1 degradation**

555 (a) Quantification of cyclin B1-Ruby degradation in control zygotes and zygotes treated with  
556 reversine averaged from 55 and 57 embryos respectively. (b) Quantification of cyclin A2-YFP  
557 degradation in control zygotes and zygotes treated with reversine averaged from 30 and 31  
558 embryos respectively. Plots in (a) and (b) show mean values +/- standard deviation.

### 559 **Figure 4**

#### 560 **Role of Emi 2 and Plk1 in the regulation of cyclin A2 and B1 degradation**

561 (a) Time between NEBD and the onset of cyclin B1-YFP degradation in zygotes injected with  
562 Emi2 MO and Emi2-5MP MO, averaged from 28 and 11 embryos respectively. The boxes  
563 show medians and the first and third quartiles. The whiskers are set at 1.5\*IQR above the  
564 third and below the first quartile. Outlier values are marked with dots. (b) Quantification of  
565 cyclin B1-Ruby degradation in control zygotes, zygotes injected with wt Plk1-YFP or kd Plk1-  
566 YFP, and zygotes treated with BI2536, a Plk1 inhibitor, averaged from 55, 38, 11 and 12  
567 embryos respectively. (c) Quantification of cyclin A2-YFP degradation in control zygotes,  
568 zygotes injected with wt Plk1-TagRFP and zygotes treated with BI2536, averaged from 30, 22  
569 and 38 embryos respectively. (d) Quantification of cyclin B1-Ruby degradation in control  
570 zygotes and zygotes treated with BI2536 or BI2536 and reversine, averaged from 55, 12, and  
571 15 embryos respectively. Plots in (b)-(d) show mean values +/- standard deviation.

572

573 **Table 1**

574 **Mitotic timings in mouse embryos injected with cyclin A2-YFP**

Experimental conditions	Total no.	Time between NEBD	Time between NEBD	
		and cyclin A2 degradation (min; median (Q1;Q3))	and anaphase (min; median (Q1;Q3))	
1-cell	control	30	39.0 (30.0 ; 54.0)	111.0 (99.8 ; 117.0)
	reversine	31	3.0 (0.0 ; 19.5) <sup>b</sup>	99.0 (93.0 ; 108.0)
	wt Plk1 OE	22	15.0 (0.0 ; 26.3) <sup>d</sup>	108.0 (105.0 ; 117.0)
	BI2536	38	-	-
2-cell	control	37	0.0 (0.0 ; 0.0) <sup>b,c,e</sup>	57.0 (51.0 ; 63.0) <sup>b,d,f</sup>

575 <sup>a</sup> p<0.05, <sup>b</sup> p<0.001 comparing to control 1-cell embryos, <sup>c</sup> p<0.05, <sup>d</sup> p<0.001 comparing to  
576 reversine-treated 1-cell embryos, <sup>e</sup> p<0.05, <sup>f</sup> p<0.001 comparing to 1-cell embryos  
577 overexpressing wt Plk1

578

579

580

581

582

583

584

585

586

587

588

589

590

591 **Table 2**

592 **Mitotic timings in mouse embryos injected with cyclin B1-Ruby**

Experimental conditions	Total no.	Time between NEBD	Time between NEBD
		and cyclin A2 degradation (min; median (Q1;Q3))	and anaphase (min; median (Q1;Q3))
control	55	48.0 (40.5 ; 52.5)	96.0 (87.0 ; 105.0)
reversine	57	39.0 (30.0 ; 45.0) <sup>b</sup>	87.0 (81.0 ; 96.0)
wt Plk1 OE	38	28.5 (24.0 ; 33.0) <sup>a</sup>	78.0 (75.0 ; 92.3) <sup>a</sup>
kd Plk1 OE	11	45.0 (39.0 ; 51.0)	87.0 (82.5 ; 99.0)
BI2536	12	93.0 (83.3 ; 100.5) <sup>b</sup>	-
1-cell BI2536 + reversine	15	90.0 (87.0 ; 103.5) <sup>b</sup>	-
1-cell cyclin A2 OE (0.07 µg/µl)	41	48.0 (45.0 ; 51.0)	115.5 (105.8 ; 128.3) <sup>a</sup>
1-cell cyclin A2 OE (0.2 µg/µl)	12	54.0 (44.3 ; 60.8)	117.0 (111.0 ; 135) <sup>e</sup>
1-cell cyclin A2 OE (0.4 µg/µl)	10	54.0 (51.8 ; 67.5)	-
2-cell control	31	18.0 (15.0 ; 24.0) <sup>a,c</sup>	76.5 (69.8 ; 81) <sup>a,d</sup>

593 <sup>a</sup> p<0.001, <sup>b</sup> p<0.05 comparing to control 1-cell embryos, <sup>c</sup> p<0.001, <sup>d</sup> p<0.05 comparing to  
 594 reversine-treated 1-cell embryos, <sup>e</sup> values calculated only for embryos that completed  
 595 cytokinesis (9 out of 12).

596

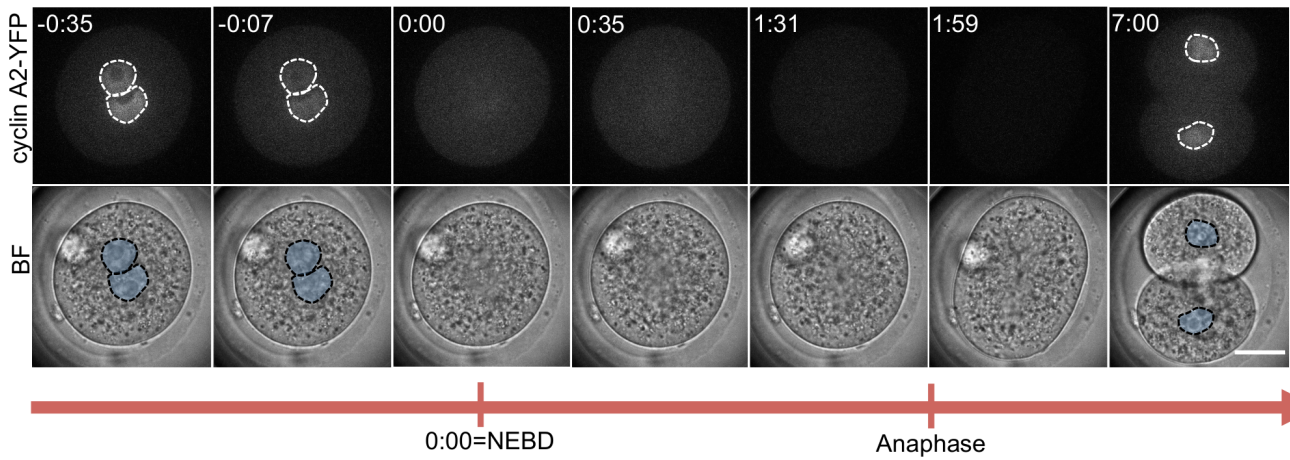
597

598

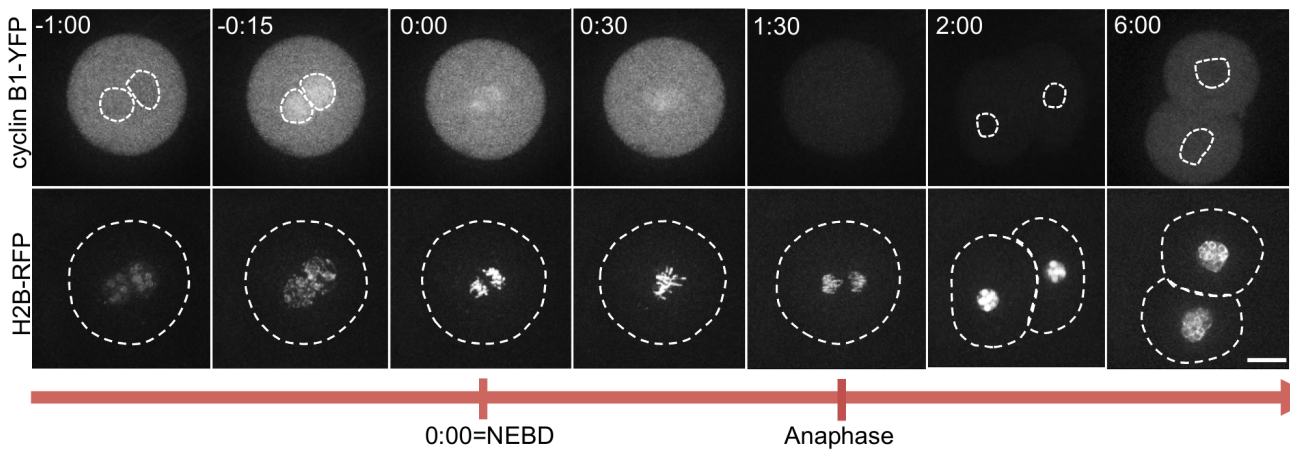
599

# Figure 1

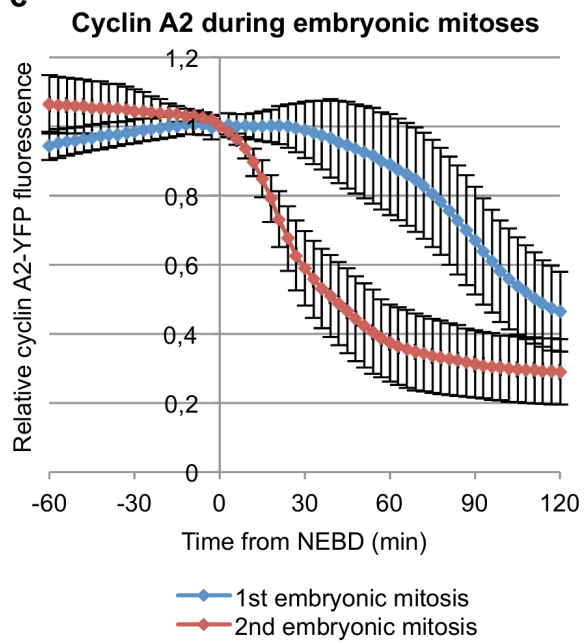
**a**



**b**



**c**



**d**

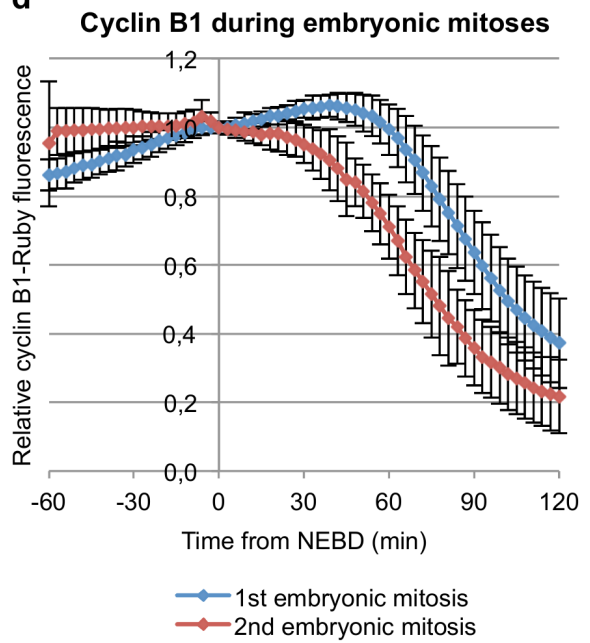
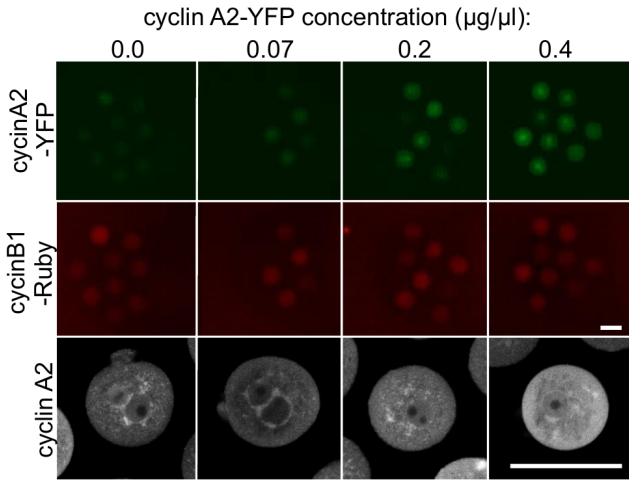
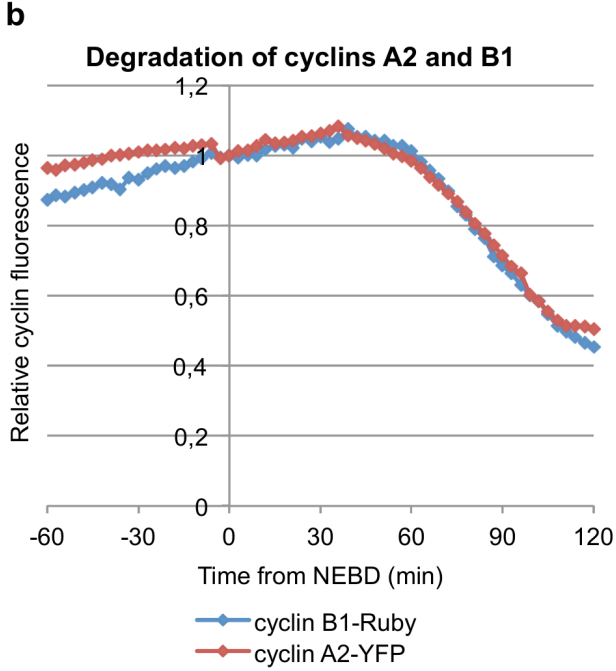
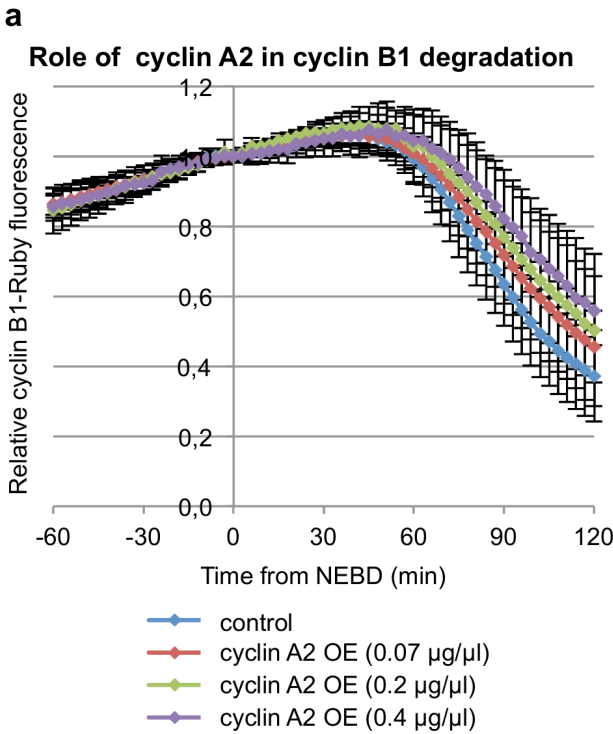




Figure 2



# Figure 3

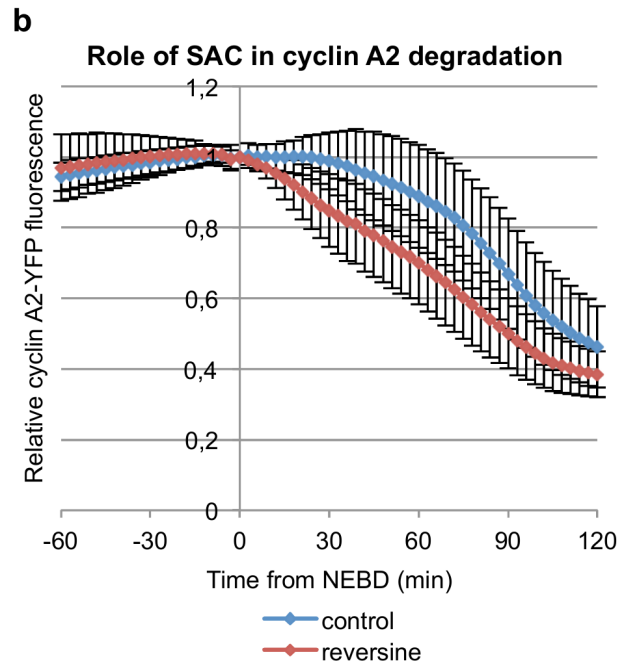
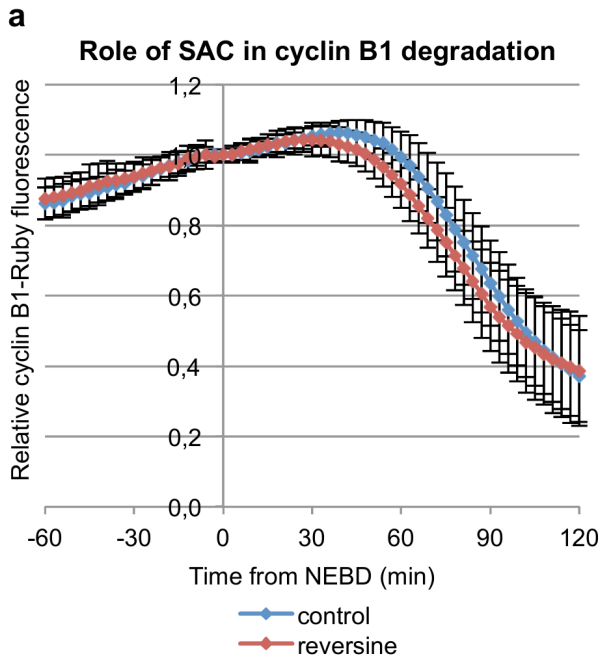


Figure 4

